Inelastic Scattering of Protons

ROBERT H. DICKE AND JOHN MARSHALL, JR.
University of Rochester, Rochester, New York

(Received December 17, 1942)

The proton energy lost in an inelastic collision with a nucleus reappears as an excitation energy of the nucleus. The measurement of the energy loss of inelastically scattered protons is a convenient method of determining the energies of nuclear excitation levels. Protons scattered at an angle of 135° by a thin scattering foil are detected by a proportional counter feeding a scaling circuit which is biased to count only the large pulses resulting from slowly moving protons. Aluminum stopping foils introduced between the scatterer and counter are used to slow down the scattered protons so that protons of a particular energy group move through the counter slowly and are counted. A plot of the number of counted protons against stopping foil thickness gives a curve in which peaks appear for different proton energy groups. Well-defined peaks corresponding to inelastically scattered protons are obtained for a number of substances and excitation energies are computed.

INTRODUCTION

IF a proton approaches a nucleus closely, any one of several things may happen. The proton may be scattered elastically so that the total kinetic energy after collision is the same as before. On the other hand, it may be scattered inelastically so that the nucleus is left in an excited state. Another possibility would be nuclear transformation induced by the proton. An example of this would be the (p, α) reaction.

Inelastic scattering can be thought of as a (p, p) reaction in which the proton enters the nucleus, and later a proton leaves it with a lower kinetic energy than that of the original proton, thus leaving the nucleus in an excited state. It has been shown that in general a (p, n) reaction is more likely to occur than a (p, p) reaction.[1] In the case of a (p, p) reaction, the proton must penetrate the Coulomb barrier in order to leave the nucleus. This is not the case for the neutron in a (p, n) reaction. Thus, if a (p, n) reaction is energetically possible, one would expect to observe very little inelastic scattering of protons. The substances most suitable for the observation of inelastic scattering then are those which have high (p, n) thresholds.

Heavy elements are, in general, unsuitable for inelastic scattering experiments because of the difficulty of penetration of the Coulomb barrier. In general, the substances most favorable for inelastic scattering are light elements with high (p, n) thresholds.

Wilkins and Kuerti,[2] Wilkins and Wrenshall,[3] and Wilkins,[4] using their photographic emulsion technique, observed the inelastic scattering of protons. From their work levels were found in Mg and Al. Their values agree fairly closely

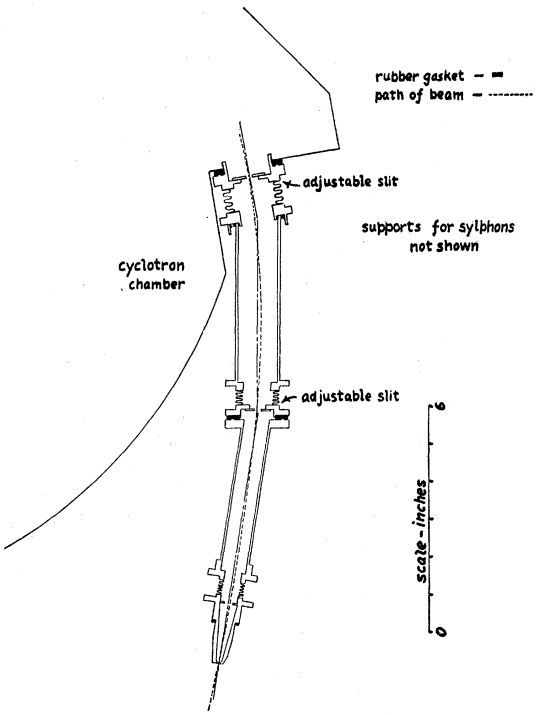

FIG. 1. Slit system.

[1] V. Weisskopf and D. Ewing, Phys. Rev. **57**, 472 (1940).

[2] T. R. Wilkins and G. Kuerti, Phys. Rev. **57**, 1082 (1940).

[3] T. R. Wilkins and G. Wrenshall, Phys. Rev. **58**, 758 (1940).

[4] T. R. Wilkins, Phys. Rev. **60**, 365 (1941).

with those given here. In the case of aluminum, there is agreement with a known γ-ray energy.

APPARATUS

The University of Rochester cyclotron gives a proton beam of approximately 6.9-Mev energy. The beam, however, is not completely homogeneous. To get a monochromatic beam of protons from the cyclotron, one may bring out the beam through a system of slits in the fringing field of the cyclotron magnet. With three slits it is possible to get as nearly monochromatic a beam as is desired by making the slits narrow enough. The system of slits used is shown in Fig. 1. The slit system is open to the cyclotron vacuum and the exit slit is covered by an aluminum window.

Figure 2 shows the scattering chamber, monitoring ionization chamber, and proportional counter used in these experiments. The foil is mounted in the center of the chamber which is evacuated to eliminate scattering from air around the foil. A small ionization chamber is mounted at the rear of the scattering chamber for the purpose of monitoring the beam. The window through which the scattered protons leave the chamber is mounted at an angle of 135° from the direction of the incident protons. It is composed of a thin aluminum foil waxed onto a supporting grid. After the scattered protons leave this window, they pass through an aluminum stopping foil and enter a proportional counter.

The proportional counter was filled to a pressure of 20 cm with commercial argon and operated a scale of 32 through a pulse amplifier. The scaling circuit could be adjusted to respond to pulses of various sizes.

There are, in general, two methods of range measurement. If the scaling circuit bias is adjusted so that all protons are counted but that the γ-ray background is not counted, we speak of the "plateau method." If the number of protons counted is plotted against absorber thickness, we obtain a step-like curve with a step at every proton energy group. If on the other hand, the bias is adjusted so that only the largest pulses are counted, we speak of the "peak method." Only very slowly moving protons can produce pulses which are large enough to be counted, and a plot of number of protons against number of absorbers gives a curve with peaks corresponding to the proton energy groups. This is illustrated in Fig. 3, which is a plot of number of recorded proton pulses against thickness of stopping foils for various scaling circuit biases.

A remote control system employing selsyn motors was used for changing the absorber foils. The absorber foils were cemented over holes around the edge of a large aluminum disk. This

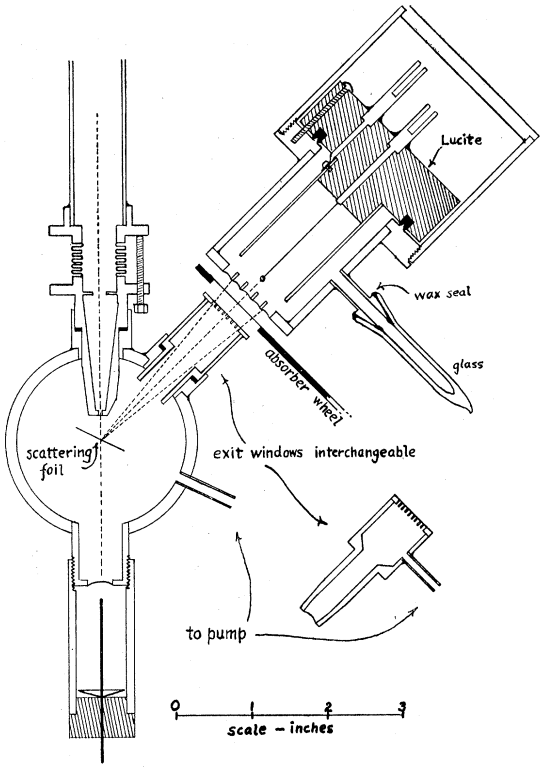

FIG. 2. Scattering chamber and counter.

disk was coaxial with a gear which was driven by a one-tooth pinion mounted on the selsyn motor shaft. Thus one revolution of the selsyn motor changed from one absorber foil to the next.

The absorber foils were calibrated by comparing their stopping power with that of air, by the use of the proportional counter as a detector. The foils were built up in multiple layers of approximately $\frac{1}{4}$ mil of aluminum foil. It was found that each of these $\frac{1}{4}$-mil absorbers was equivalent to 1.10 cm of air at 15°C and 760 mm of mercury. Proton energies were

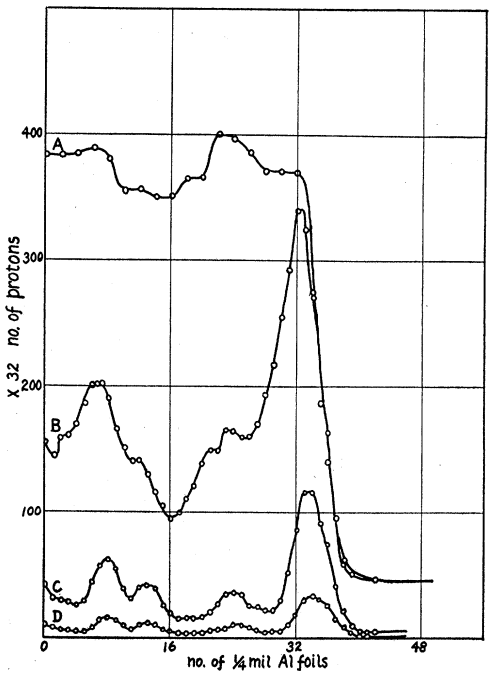

FIG. 3. Effect of scaling circuit bias on scattering curves of aluminum.

calculated from their ranges in aluminum and Livingston and Bethe's curves.[5]

RESULTS

Figure 4 is a plot of protons scattered by a Pt foil. As would be expected, there are no inelastic peaks observable. The background to the left of the elastic peak is probably due to coincidence between two small proton pulses giving the effect of a large one. The ordinate in this and the following curves if multiplied by 32 gives the total number of protons counted for any one point.

Aluminum

Figure 5 shows the scattering curve for a 0.35-mil Al foil. As can be seen, there are four peaks visible. The energy of the elastic peak was calculated from the known energy of the beam, correcting for the recoil of the nucleus. The beam energy was measured as 6.9 Mev by its range in air. Thus, the elastic peak for Al^{27} when protons are scattered at an angle of 135°, becomes 6.08 Mev.

[5] M. S. Livingston and H. A. Bethe, Rev. Mod. Phys. 9, 268 (1937).

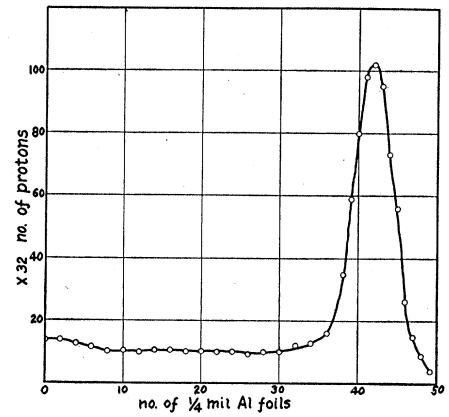

FIG. 4. Platinum scattering curve.

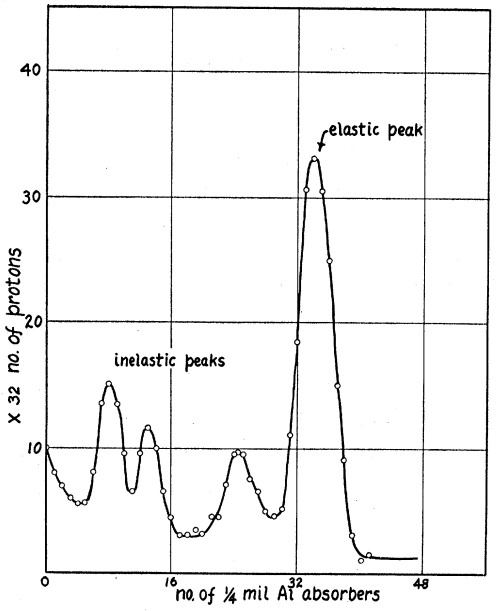

FIG. 5. Aluminum scattering curve.

TABLE I. Al^{27} scattering.

Run	Elastic peak energy Mev	Inelastic peaks I	II	III	IV
1	6.08	5.28	4.22	3.68	—
2	6.08	5.21	4.13	3.48	—
3	6.08	5.24	4.21	3.46	—
4	6.08	5.31	4.23	3.51	2.8
5	6.08	5.27	4.10	3.44	—
6	6.08	5.26	4.16	3.54	2.85
7	6.08	5.26	4.22	3.65	—
8	6.08	5.28	4.15	3.60	—
Average E	6.08	5.26	4.18	3.55	2.8
$6.08-E=\Delta$	0	0.82	1.90	2.53	3.3
Excitation energy Mev		0.87	2.03	2.70	3.5

Using the calculated value for the energy of the protons of the elastic peak, the air equivalence of our stopping foils, and Livingston and Bethe's range energy curves for air, we were able to compute the energies of the protons corresponding to the inelastic peaks. Table I shows a collection of the results of a number of scattering experiments. The first column contains the calculated values of the elastic peak. The other columns are the observed energies of the inelastic peaks. In two cases we are able to observe a fourth inelastic peak. The value for the energy of the fourth peak is rather questionable. From the observed energies of the elastic and inelastic peaks, it is possible to compute the nuclear excitation energies corresponding to these peaks. In this computation, correction was made for the difference in recoil energy of the nucleus in the case of elastic and inelastic scattering. The excitation energies for the nucleus are shown at the bottom of the table.

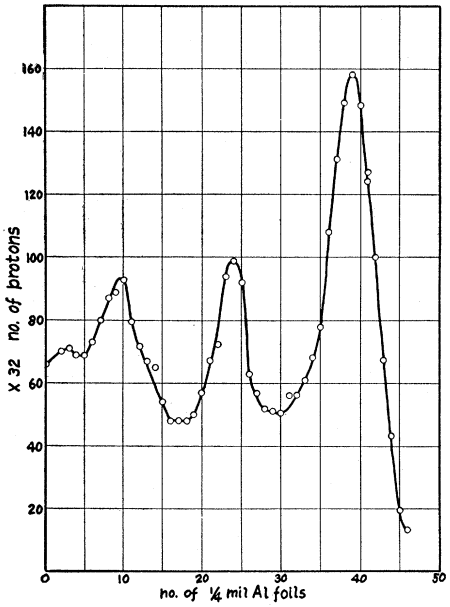

FIG. 6. Chromium scattering curve.

TABLE II. Cr^{52} scattering.

Run	Elastic peak energy Mev	Inelastic peaks I	II	III
1	6.46	5.15	3.70	—
2	6.46	5.21	3.74	2.9
Average	6.46	5.18	3.72	2.9
Δ	0	1.28	2.74	3.6
Excitation energy Mev		1.32	2.84	3.7

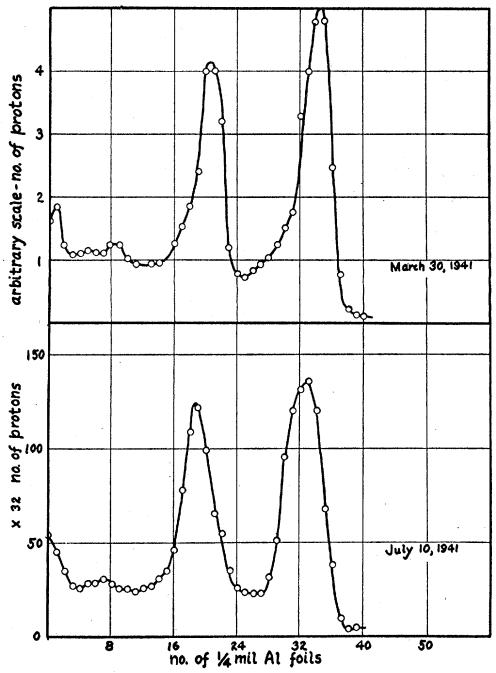

FIG. 7. Magnesium scattering curves.

TABLE III. Mg scattering.

Run	Elastic peak energy Mev	Inelastic peaks I	II	III
1	5.98	4.77	3.45	2.38
2	5.98	4.73	3.38	2.40
3	5.98	4.75	3.5	—
Average	5.98	4.75	3.44	2.39
Δ	0	1.23	2.54	3.59
Excitation energy Mev		1.32	2.74	3.88

Chromium

Figure 6 shows a scattering curve for Cr^{52}. As in the previous case, this curve shows both elastic and inelastic peaks. The foil was made by electroplating Cr on copper. The copper base was then dissolved away with concentrated nitric acid. We are very grateful to Dr. Flagg of the Chemistry Department for making these foils for us. The results of the Cr^{52} runs are shown in Table II.

Magnesium

Figure 7 shows a scattering curve for Mg. It is to be noted that the first inelastic peak is

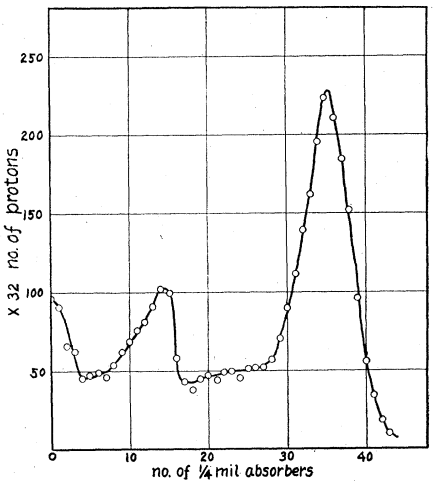

FIG. 8. Sulphur scattering curve.

almost as large as the elastic peak. There are two other observable peaks. The scattering foils used were 0.4 and 0.6 mil thick. They were obtained by rolling magnesium ribbon under oil. The results are shown in Table III. There is some doubt that all the excitation levels can be assigned to Mg^{24} since Mg^{25} and Mg^{26} have abundances of about 11 percent.

Sulphur

Figure 8 shows a scattering curve for S^{32}. Sulphur foils were prepared by rolling plastic sulphur between sheets of tantalum.

The foils obtained are quite small and a special technique was necessary to hold them in the beam. A pyroxylin film was laid down on water and the sulphur foil dropped on top before the film had hardened. This would break the film so that when it hardened it would adhere only to the edges of the foil. The film and enclosed foil were then removed on a wire frame which could be mounted in the scattering chamber. The results are given in Table IV.

A number of other elements were investigated, among them were Cu, Ni, Zn, A, Ag, N, and O. No conclusive evidence for inelastic peaks was obtained. In Zn there seemed to be faint evidence of inelastic peak structure, but this evidence was not considered good enough to warrant inclusion in these data. The reason for these negative results is probably found in the strong competition of other processes as (p, n) or (p, γ).

It would have been desirable to try a number of other elements. Among the desirable elements are Si, Na, Ne, P, and Cl. These should almost certainly yield results because of the high instability of the product nucleus of a (p, n) reaction in each case. They were not tried because of the difficulty of preparing good scattering samples.

TABLE IV. S^{32} scattering.

Run	Elastic peak energy Mev	Inelastic peaks I	III
1	6.2	4.35	2.57
2	6.2	4.32	2.57
Average	6.2	4.34	2.57
Δ	0	1.86	3.63
Excitation energy Mev		2.25	4.34

The authors wish to express their appreciation to the members of the University of Rochester Physics Department for helpful advice and criticism.